

Cookeite with a Perfect Regular Structure, Formed by Bauxite Alteration

ZOYA V. VRUBLEVSKAJA, IGOR S. DELITSIN, BORIS B. ZVYAGIN,
AND SVETLANA V. SOBOLEVA

*Institute of Geology of Ore Deposits, Petrography, Mineralogy, and Geochemistry
Academy of Science of the U.S.S.R., Moscow, U.S.S.R.*

Abstract

A di,triocahedral Li-chlorite cookeite $(\text{Li}_{0.7}\text{Al}_{2.1})_{2.8}(\text{Al}_{1.86}\text{Fe}_{0.04}^{2+}\text{Fe}_{0.09}^{3+})_{1.99}[\text{Si}_{3.38}\text{Al}_{0.62}]_{4.0}\text{O}_{10.36}(\text{OH})_{7.66}$, with an exceptionally perfect crystal structure has been found in bauxite of Djalair (Middle Asia). High-voltage diffraction (oblique-texture) patterns were used for its structural identification. It was established that it is a one-layer triclinic polytype $|\sigma_6^{\prime}\sigma_6^{\prime}|\tau_+\tau_+|\sigma_6^{\prime}\sigma_6^{\prime}| \dots$ with symmetry $C\bar{1}$ and unit cell: $a = 5.14$, $b = 8.90$, $c = 14.15$ Å, $\alpha = 90^{\circ}33'$, $\beta = 96^{\circ}12'$, $\gamma = 90^{\circ}$. The small deviation of α from 90° results in very peculiar features of the diffraction patterns, giving the false impression of a monoclinic lattice but with two non-selfconsistent β -values.

The formation of the cookeite investigated is the final result of a peculiar transformation of bauxite rock following an intermediate stage of formation of a two-layer monoclinic pyrophyllite polytype.

Introduction

Unlike triocahedral chlorites, dioctahedral and di,triocahedral varieties are much less abundant and are therefore of great interest in the crystal chemistry and genesis of minerals. In this respect the di,triocahedral Li-chlorite cookeite, found in bauxites of Djalair (Middle Asia), is especially remarkable. This chlorite, belonging to the concluding stage of a peculiar transformation process in bauxite rock, proved to be unique in its high degree of structural order, which permitted its polytype identification.

Environmental Conditions

The bauxite of the Djalair deposit is interbedded between the Upper and Lower Carboniferous in the zones of the terrestrial break. Limestones, underlying bauxite, underwent some karst development. The resultant small cavities were later filled with bauxite matter. In areas of intense karstification sheet-like bodies of bauxite occur, but these completely thin out as undissolved limestone is approached. Subsequently, the bauxite series was overlain by younger middle Carboniferous limestone.

Later the whole rock series was metamorphosed. As a result limestone was marmorized while bauxite was partly converted to emery. At present the bauxite bed forms a number of disconnected areas with a thickness of up to 3 m. In one such area, near its

lower contact (in a zone up to 0.4 m thick), the bauxite bed is broken into blocks up to 0.1 m in size. The joints between the blocks are filled with pyrophyllite. In some cases the development of pyrophyllite is so intensive that blocks of bauxite, partly transformed into emery, appear to be enclosed in cells of a pyrophyllite net.

Specimens of brown bauxite with compact shot texture from this area, kindly provided by A. P. Gapeev, contain scaly aggregates of greenish pyrophyllite. The pyrophyllite flakes, up to 4 mm in length, are usually arranged normal to the selvage joints. According to electron diffraction oblique texture patterns, the pyrophyllite belongs to the widespread $2M$ -modification $\sigma_3\sigma_3\tau_1\sigma_3\sigma_3\tau_5\sigma_3\sigma_3$ (Zvyagin, Mischenko and Soboleva, 1968). Distinct, weak, glide surfaces or zones developed in the pyrophyllite, commonly along an oblique direction relative to the long axes of the scaly pyrophyllite aggregates. The material filling these zones strongly differs from the pyrophyllite both in color (white or bluish gray) and texture (from fine-grained to macrocrystalline). Exceptionally good electron diffraction texture patterns with a great number of very clear, sharp, and well resolved reflections have been obtained for this material. The analysis of the reflection set has indicated that the specimen is a di,triocahedral chlorite with a regular structure indicative of a definite polytype.

Chlorite Polytypes

Since chlorite structures consist of two kinds of alternating layers, which may have different relative displacements and orientations, an enormous variety of polytypes is possible. All these polytypes can be divided into six groups differing by the projection on the plane ac of the *chlorite packet* (=repeating combination of layers). These groups have been designated by Bailey and Brown (1962) as $Ia-2n$, $Ib-2n$, $IIb-(2n + 1)$, $IIa-2n$, $IIa-(2n + 1)$, $IIb-2n$, where $1 \leq 2n$, $2n + 1 \leq 4$. Zvyagin (1967) has used for these groups designations σ , σ' , $|\sigma|$, $|\sigma'|$, $|\sigma|, |\sigma'|$, here σ being a general symbol for intersheet displacements in an 2:1 layer. A prime or its absence indicates the relative orientation of octahedral sheets of both layers of the packet: in packet σ' they have the same orientation and in packet σ , opposite orientations. The vertical line indicates a superposition of octahedral cations of the hydroxide layer and of the adjacent tetrahedral cations in the normal projection on the ab plane. Within each of the six groups, the polytype structures differ by intersheet and interlayer displacements of $\pm b/3$ along the b axis.

If these displacements are randomly distributed, Bailey and Brown (1962) call the corresponding polytypes "semirandom." For any of the polytype groups there is one semirandom polytype with the same designation. Natural chlorites are usually semirandom, the σ -polytype being more abundant. Semirandom polytypes with packet $\sigma', \sigma', |\sigma'|$ are more rare, while those with packets $|\sigma|, \sigma$ have never been found.

Regular polytypes have quite definite intersheet displacements differing by components along axes a, b of their normal projection on plane ab , specified by subscripts $i = 1, 2 \dots 6$ and $+, -, 0$ (Zvyagin, 1967). In addition to displacements σ inside the 2:1 layer, the displacement τ between adjacent sheets belonging to different layers must be specified. For a trioctahedral hydroxide layer, τ is measured between the origins of the tetrahedral sheets adjoining the intermediate hydroxide layer. Any chlorite structure may be thus described by a succession of letters σ, τ with conventional marks and subscripts.

Regular polytypes are rather rare. Usually they appear in single crystals and are more probable for dioctahedral and di, trioctahedral chlorites because trioctahedral varieties are less sensitive to displacements ($\pm b/3$) along the b axis. Table 1 lists all regular polytypes known to date including the cookeite under study. For each polytype the symbolic notation, mode of octahedral population, number of layers per

unit cell, space group symmetry, and components (x_n, y_n) of the c axis in normal projection on the ab plane are indicated.

Electron Diffraction Features of Chlorite Polytypes

In the course of electron diffraction study of layer silicates, samples of dioctahedral and di, trioctahedral chlorites from different deposits of the USSR and other countries have been identified and examined. According to the intensities of the $k = 3n$ reflections, most of these chlorites consist of packets $|\sigma'|$, the others consisting of packets σ . The $k \neq 3n$ reflections that indicate 3-dimensional structural regularity, though sometimes present on the patterns, were insufficient for unequivocal identification of polytypes. In contrast the chlorite from the bauxite of Djalaïr has a much more regular structure, and its oblique texture patterns (Fig. 1) offered a favorable opportunity for a precise analysis of the lattice geometry and a reliable polytype identification.

Lattice Geometry of the Cookeite

The geometry of texture patterns might appear at first glance to satisfy the "monoclinic" arrangement of reflections. In a monoclinic case the heights D —namely, the distances of reflections from the minor axis of the ellipses, these distances being proportional to the projections of reciprocal lattice vectors $[hkl]$ on the c^* axis—depend only on indices h, l because $D = hp + lq$ where $p \sim a^* \cos \beta^*$, $q \sim c^*$. The reflections $02l, 11l$ are disposed non-uniformly along the first ellipse in the patterns of the chlorite studied, while the $20l, 20l, 13l, 13l$ reflections of the second ellipse are grouped in compact sets of four reflections (Zvyagin *et al.*, 1972). Such peculiarities usually mean that p differs from $q/3$ —that is, p/q differs from $1/3$ —to the extent that β deviates from its ideal value. The real D values have indicated, however, that the ratios p/q , determined separately from the first and second ellipse, are non-equal, the first (0.305) being smaller and the second (0.375) being greater than $1/3$. These two p/q ratios lead to two different β values having opposite deviations from the ideal β value, for which $p/q = 1/3$ and $c \cdot \cos \beta / a = -1/3$. To resolve this paradox, the heights D for the second ellipse reflections were calculated by use of p and q values determined from the heights D of the first ellipse reflections, and then compared with the experimental values. As it turned out, the inner and the outer reflections of the above mentioned sets of four reflections essentially differ by degree of agreement of

TABLE 1. Experimentally Identified Regular Chlorite Polytypes

N	Number of packets / repeat	Ideal symmetry	Symbolic notation according to Zvyagin (1967)	Symbolic notation according to Bailey, Brown (1962) and Lister, Bailey (1967)	x_n, y_n	Sample name	Di- or Trioctahedral	Reference
1	1	$C2/m$	$\sigma_6 \tau_6 \sigma_6$	\bar{x}_1 -IIb-2 {IIb-2}	-1/3,0	pennine B prochlorite	T T	B S
2	1	$C\bar{1}$	$\sigma_2 \tau_4 \sigma_2$ ($\sigma_6 \tau_2 \sigma_6$)	\bar{x}_2 -IIb-6 (\bar{x}_1 -IIb-4 {IIb-4})	-1/3,0 (-1/3,-1/3)	chlorite pennine A chlorite	T T T	Z B S
3	2	$C2/c$	$\sigma_3 \tau_1 \sigma_3 \tau_5 \sigma_3$ ($\sigma_6 \tau_4 \sigma_6 \tau_2 \sigma_6$)	x_1 -Ib-3: x_1 -Ib-5 (\bar{x}_1 -IIb-6: \bar{x}_1 -IIb-4)	-1/3,0 (1/3,0)	donbassite	D-T	DL
4	2	$C\bar{1}$	$\sigma_3 \tau_5 \sigma_3 \tau_5 \sigma_3$ ($\sigma_6 \tau_2 \sigma_6 \tau_2 \sigma_6$)	x_1 -Ib-5: x_2 -Ib-5 (\bar{x}_1 -IIb-4: \bar{x}_2 -IIb-4)	-1/3,0 (1/3,0)	chlorite C	T	B
5	3	$C\bar{1}$	$\sigma_3 \tau_3 \sigma_1 \tau_5 \sigma_1 \tau_3 \sigma_3$ ($\sigma_6 \tau_6 \sigma_4 \tau_2 \sigma_4 \tau_6 \sigma_6$)	x_1 -Ib-1: x_2 -Ib-5: x_3 -Ib-1 (\bar{x}_1 -IIb-2: \bar{x}_3 -IIb-4: \bar{x}_3 -IIb-2)	0,-1/3 (0,1/3)	chlorite D	T	B
6	1	$C2$	$\left \begin{matrix} \sigma_3 & \tau_+ & \sigma_3 \\ \sigma_6 & \tau_- & \sigma_6 \end{matrix} \right $	x_1 -IIa-1 (\bar{x}_1 -Ia-2 {Ia-2})	-1/3,0 (1/3,0)	donbassite	D	DA
7**	1	$C\bar{1}$	$\left \begin{matrix} \sigma_6 & \tau_- & \sigma_6 \\ \sigma_4 & \tau_+ & \sigma_4 \end{matrix} \right $ $\left \begin{matrix} \sigma_5 & \tau_+ & \sigma_5 \\ \sigma_6 & \tau_- & \sigma_6 \end{matrix} \right $	\bar{x}_1 -Ia-4 {Ia-4} (x_3 -IIa-1) x_2 -IIa-1 (\bar{x}_1 -Ia-6 {Ia-6})	1/3,-1/3 (-1/3,0) -1/3,0 (1/3,1/3)	Cr-chlorite cookeite	T D-T	BB This
8	2	$C2/c$	$\left \begin{matrix} \sigma_6 & \tau_- & \sigma_6 & \tau_+ & \sigma_6 \\ \sigma_6 & \tau_+ & \sigma_6 & \tau_- & \sigma_6 \end{matrix} \right $	\bar{x}_1 -Ia-4: \bar{x}_1 -Ia-6	-1/3,0	cookeite 2 vermiculite „s”	D-T T	LB MW
9***	2	Cc	$\left \begin{matrix} \sigma_4 & \tau_- & \sigma_5 & \tau_+ & \sigma_4 \\ \sigma_6 & \tau_+ & \sigma_4 & \tau_- & \sigma_6 \end{matrix} \right $ $\left \begin{matrix} \sigma_4 & \tau_+ & \sigma_5 & \tau_- & \sigma_4 \\ \sigma_6 & \tau_- & \sigma_4 & \tau_+ & \sigma_6 \end{matrix} \right $ $\left \begin{matrix} \sigma_4 & \tau_+ & \sigma_2 & \tau_- & \sigma_4 \\ \sigma_6 & \tau_+ & \sigma_4 & \tau_- & \sigma_6 \end{matrix} \right $ $\left \begin{matrix} \sigma_6 & \tau_+ & \sigma_2 & \tau_- & \sigma_6 \\ \sigma_2 & \tau_+ & \sigma_4 & \tau_- & \sigma_2 \end{matrix} \right $	x_3 -IIa-5: x_2 -IIa-3 (\bar{x}_1 -Ia-6: \bar{x}_3 -Ia-2) x_3 -IIa-1: x_2 -IIa-1 (\bar{x}_1 -Ia-4: \bar{x}_3 -Ia-4) \bar{x}_3 -Ia-2: \bar{x}_2 -Ia-2 (\bar{x}_1 -Ia-4: \bar{x}_3 -Ia-4) \bar{x}_1 -Ia-6: \bar{x}_2 -Ia-6 (\bar{x}_2 -Ia-2: \bar{x}_3 -Ia-2)	1/3,0 (-1/3,1/3) 1/3,0 (-1/3,1/3) -1/3,0 (-1/3,1/3) -1/3,-1/3 (-1/3,0)	vermiculite „q” vermiculite „r” donbassite cookeite 1	T T D D-T	MW MW DL LB
10	2	Cc	$\left \begin{matrix} \sigma_6 & \tau_2 \sigma_5 & \tau_3 \sigma_6 \\ \sigma_5 & \tau_1 \sigma_4 & \tau_2 \sigma_5 \end{matrix} \right $	\bar{x}_1 -Ia-3: x_2 -IIa-6 (x_2 -IIa-2: \bar{x}_3 -Ia-1)	0,0 (0,0)	Cr-chlorite	T	LB

B = Brindley et al, 1950
 BB = Brown, Bailey, 1963
 DA = Drits, Alexandrova, 1967
 DL = Drits, Lasarenko, 1967
 LB = Lister, Bailey, 1967

MW = Mathieson, Walker, 1954
 S = Steinfink, 1958
 SB = Shirozu, Bailey, 1966
 This = This work
 Z = Zvyagin, 1963

* To simplify the designations of centrosymmetric 2:1 layer single symbols σ_i instead of double symbols $\sigma_i \sigma_i$ are used. In parentheses alternative notations are given which correspond either to an orientation \bar{x}_1 of the first layer or to a cell with only one oblique angle α or β (y_n or $x_n = 0$).

** Both structures are connected by a reflexion in a plane normal to the b -axis or by 180° -rotation around the b -axis.

*** All these four structures (composition differences being neglected) are in fact congruent. After rotation by 180° around c the structures with even subscripts σ_i became equivalent to vermiculite „r”, which in its turn transfers into vermiculite „q” after rotation by 180° around the b -axis combined with a translation $c/2$.

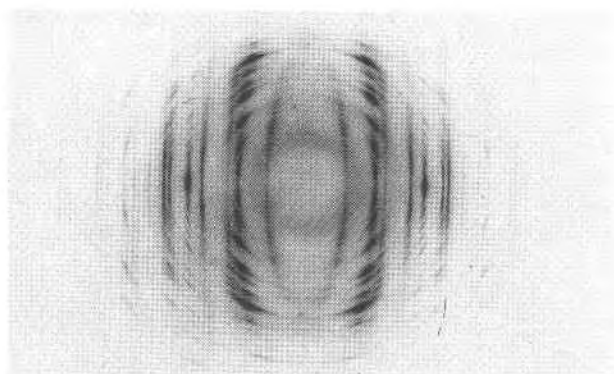


FIG. 1. Electron diffraction oblique texture pattern of the Djalair cookeite (inclination angle $\phi = 70^\circ$).

calculated and measured D values. Taking into account that the reflections of the second ellipse have the hk indices 20 , $\bar{2}0$, 13 , or $\bar{1}3$, one can conclude that such a discrepancy is due to a small "triclinic" distortion of the lattice ($\alpha \neq 90^\circ$). As a consequence not only $p \neq 0$ but also $s \sim b^* \cdot \cos \alpha^* \neq 0$, so that in fact $D = hp + ks + lq$. This distortion does not affect the positions of the $k = 0$ reflections but its influence on the positions of the $k \neq 0$ reflections becomes more pronounced as k increases. The splitting of the $k \neq 0$ reflections must lead in principle to an increase of the number of reflections in an interval $\Delta D = q$, but if s is small, this may not be revealed. If $|F_{hkl}| \ll |F_{\bar{h}\bar{k}l}|$, the inequality $s \neq 0$ is manifested only by small displacements of reflections against their theoretical "monoclinic" positions. For this reason the heights D of the first ellipse reflections ($k = 1, 2$) lead to rough but yet reliable—at least concerning the relation p/q —values p, q . The values of p, q so obtained indicate $p/q < 1/3$. Therefore in the "monoclinic" sets of four reflections on the second ellipse, the outer reflections must have indices $13l$, $\bar{1}.3.l+1$, while the inner ones have indices $\bar{2}.0.l+1$, $20l$. If $s \neq 0$, each reflection $13l$, $\bar{1}3l$, $1\bar{3}l$, $\bar{1}\bar{3}l$ splits into two reflections with opposite signs of k , one moving away from and the other toward a $20l$ reflection by a value $\Delta D = 3s$. As a result the number of reflections in each set increases from 4 to 6. To see all of them separately, sufficient resolution is needed. Otherwise the close pairs of reflections appear to be single reflections and give the impression of a monoclinic structure. It is easy to show that for any $p = q/3 + \delta$ a complete coincidence of these reflections takes place if $s = \pm\delta$, where δ may be both $>$ and $<$ 0. The heights of the second ellipse reflections give a reliable q value and an apparent value $p' = q/3 - \delta'$, where $\delta' = 2\delta$. Both by positions and intensities, the single reflections $13l$, $\bar{1}3l$, $1\bar{3}l$, $\bar{1}\bar{3}l$ seem to be "monoclinic" $20l$ and the coin-

cing reflections of the sets seem to be "monoclinic" $13l$, $\bar{1}3l$, $1\bar{3}l$, $\bar{1}\bar{3}l$ (Zvyagin *et al.*, 1972).

The fact that only four reflections are distinguished in a set on the second ellipse is not yet complete evidence on an exact coincidence of the approached reflections. Therefore further analysis of the patterns should be based on the outer reflections $1\bar{3}l$, $\bar{1}.3.l+1$ of the sets. These are single and their situations can be measured with accuracy. Using the heights D of these reflections, a more exact value q may be calculated, for example by means of the relations $q = (D_{1\bar{3}l} + D_{\bar{1}.3.l+1})/(2l + 1)$. Thereupon measuring the splitting of $0kl, 0\bar{k}l$ reflections adjacent to levels $D + lq$ —this splitting is more pronounced for reflections $04l, 0\bar{4}l$ of the third ellipse—one may establish the s value as $s = (D_{0kl} - D_{0\bar{k}l})/2k$. With q and s known, the value of p can be obtained by using the non-coinciding reflections of the second ellipse. Thus the height difference ΔD of the outer reflections for each set of six reflections is equal to $q + 6s - 2p$ and hence $p = (q + 6s - \Delta D)/2$.

In such a way the following relations have been obtained: $p = 0.297q$, $\delta = -0.036q$, $s = 0.016q$, $s = -0.45\delta$, to which a unit cell corresponds: $a = 5.14$, $b = 8.90$, $c = 14.15 \text{ \AA}$, $\alpha = 90^\circ 33'$, $\beta = 96^\circ 12'$, $\gamma = 90^\circ$. This chlorite is thus triclinic and contains one packet per repeat c . Low values for a and b as well as the intensity relation of the reflections of the sixth ($26l$, $40l$) and seventh ($17l$, $35l$, $42l$) ellipses indicate that it may be di- or dioctahedral. In fact the structural formula $(\text{Li}_{0.7}\text{Al}_{2.1})_{2.8}(\text{Al}_{1.86}\text{Fe}_{0.04}^{2+}\text{Fe}_{0.09}^{3+})_{1.99}[\text{Si}_{3.38}\text{Al}_{0.62}]_{4.0}\text{O}_{10.35}(\text{OH})_{7.65}$, calculated from the chemical analyses (Table 2), corresponds to cookeite with a dioctahedral 2:1 layer (the degree of octahedral occupancy 1.99) and an almost trioctahedral hydroxide interlayer sheet (the degree of occupancy 2.8).

TABLE 2. Chemical Analysis of Djalair Cookeite*

	Wt per cent
SiO_2	38.26
Al_2O_3	44.28
Fe_2O_3	1.31
FeO	0.48
Li_2O	2.00
H_2O^+	13.00
Total	99.33

*Analyst R.L. Teleshova

The Polytype Identification of the Cookeite

According to the intensities of the second ellipse reflections (Table 3), the structure of this cookeite consists of packets $|\sigma'|$. Only three one-packet polytypes from di- and di,triectahedral packets satisfying the uniformity condition are possible, namely $|\sigma'_3\sigma'_3| \tau_0\tau_0 | \sigma'_3\sigma'_3|$, $|\sigma'_3\sigma'_3| \tau_+\tau_- | \sigma'_3\sigma'_3|$, $|\sigma'_5\sigma'_5| \tau_+\tau_+ | \sigma'_5\sigma'_5|$ with corresponding symmetry $C2/m$, $C2$, $C\bar{1}$. Only the one with symmetry $C2$ has been

TABLE 3. Second Ellipse Reflections for Trioctahedral and Di,triectahedral Chlorites from Packets $|\sigma'|$ at $p/q = 1/3$, $s = 0$ and at $p/q = 1/3 - 0.036$, $s/q = 0.016$

hkl	D/q ($p/q = 1/3$, $s = 0$)	F^2_{tri}	F^2_{di-tri}	D/q ($p/q = 0.297$, $s = 0.016$)	d	F^2_{calc}	F^2_{exp}
130	1/3	68	129	0.25	2.598	27	20
130				0.35	2.566	27	150
201				0.40	2.564	75	
200	2/3	158	152	0.60	2.556	80	155
131				0.65	2.552	36	
131				0.75	2.546	36	
131	4/3	135	185	1.25	2.506	75	140
131				1.35	2.496	75	220
202				1.40	2.491	35	
201	5/3	113	142	1.60	2.461	30	30
132				1.65	2.459	56	28
132				1.75	2.448	56	
132	7/3	1	15	2.25	2.378	3	2
132				2.35	2.361	3	6
203				2.40	2.351	9	
202	8/3	855	855	2.60	2.323	315	300
133				2.65	2.312	270	135
133				2.75	2.258	270	
133	10/3	23	33	3.25	2.210	9	20
133				3.35	2.193	9	45
204				3.40	2.181	15	
203	11/3	11	13	3.60	2.147	7	10
134				3.65	2.138	3	15
134				3.75	2.120	3	
134	13/3	57	33	4.25	2.029	8	15
134				4.35	2.013	8	44
205				4.40	2.002	17	
204	14/3	332	364	4.60	1.969	78	180
135				4.65	1.957	93	130
135				4.75	1.941	93	
135	16/3	3	10	5.25	1.855	3	3
135				5.35	1.839	3	2
206				5.40	1.828	4	
205	17/3	9	8	5.60	1.797	0	2
136				5.65	1.788	4	50
136				5.75	1.772	4	
136	19/3	34	63	6.25	1.693	26	55
136				6.35	1.679	26	180
207				6.40	1.670	11	
206	20/3	640	504	6.60	1.642	136	120
137				6.65	1.632	184	50
137				6.75	1.619	184	
137	22/3	146	125	7.25	1.548	50	70
137				7.35	1.536	50	9
208				7.40	1.527	25	
138	23/3	17	21	7.60	1.503	15	25
138				7.65	1.495	4	50
138				7.75	1.482	4	
138	25/3	51	44	8.25	1.421	10	20
138				8.35	1.410	10	7
209				8.40	1.403	24	
208	26/3	17	8	8.60	1.381	2	100
139				8.65	1.373	3	170
139				8.75	1.363	3	
139	28/3	495	363	9.25	1.309	130	71
139				9.35	1.299	130	25
210				9.40	1.293	104	
139	29/3	73	67	9.60	1.273	17	25
139				9.65	1.268	25	25
139				9.75	1.258	25	

TABLE 4. Distinguishing Diffraction Features of Three Di,triectahedral Chlorite Polytypes from Packets $|\sigma'|$, Represented by the First Ellipse Reflections

hkl	D/q ($p/q = 1/3$, $s = 0$)	F^2_{calc} $C2/m$	$C2$	D/q ($p/q = 0.297$, $s/q = 0.016$)	d	F^2_{calc} $C\bar{1}$	F^2_{exp}
020	0	580	380	-0.032	4.450	0.2	114
020				0.032	4.450	0.2	
110	1/3	112	42	0.28	4.433	0.2	116
110				0.31	4.428	130	
111	2/3	166	72	0.69	4.349	170	95
111				0.72	4.340	25	
021	1	40	127	0.97	4.256	70	170
021				1.03	4.231	80	
111	4/3	15	86	1.28	4.124	220	44
111				1.31	4.109	19	
112	5/3	240	420	1.69	3.926	16	110
112				1.72	3.910	12	
022	2	14	68	1.97	3.778	182	85
022				2.03	3.744	18	
112	7/3	32	106	2.28	3.609	45	149
112				2.31	3.591	58	
113	8/3	84	34	2.69	3.391	12	79
113				2.72	3.374	104	
023	3	52	18	2.97	3.245	0.2	77
023				3.03	3.198	64	
113	10/3	248	152	3.28	3.088	0.0	73
113				3.31	3.071	0.6	
114	11/3	50	18	3.69	2.897	0.4	76
114				3.72	2.882	43	
024	4	74	34	3.97	2.774	6	89
024				4.03	2.746	53	
114	13/3	6	36	4.28	2.645	23	4
114				4.31	2.631	24	
115	14/3	1	18	4.69	2.489	66	75
115				4.72	2.746	4	
025	5	56	104	4.97	2.390	2	70
025				5.03	2.368	6	
115	16/3	3	21	5.28	2.285	9	73
115				5.31	2.275	42	
116	17/3	12	32	5.69	2.161	6	77
116				5.72	2.152	13	
026	6	16	5	5.97	2.083	29	71
026				6.03	2.066	1	
116	19/3	7	2	6.28	2.001	13	73
116				6.31	1.993	0.5	

recognized among the natural chlorites (Drits and Alexandrova, 1968, Table 1). The $|F|^2$ values calculated for these structures using the first ellipse reflections—namely, $11l$, $\bar{1}\bar{1}l$, $1\bar{1}l$, $\bar{1}1l$, $02l$, $0\bar{2}l$ —compared to those observed (Table 4) indicate that the cookeite studied has the triclinic ($C\bar{1}$) structure ($|\sigma'_5\sigma'_5| \tau_+\tau_+ | \sigma'_5\sigma'_5|$). The same structure after rotation by 180° around the b axis would have a notation $|\sigma'_1\sigma'_1| \tau_-\tau_- | \sigma'_1\sigma'_1|$, but it should be taken into account that in this case $s < 0$, $\alpha < 90^\circ$.

After the polytype identification of Djalair cookeite, it becomes possible to recognize the features of this polytype (Fig. 2) in the less perfect electron diffraction oblique texture patterns of some other chlorites. This gives an indication of the natural abundance as well as of the crystallochemical and

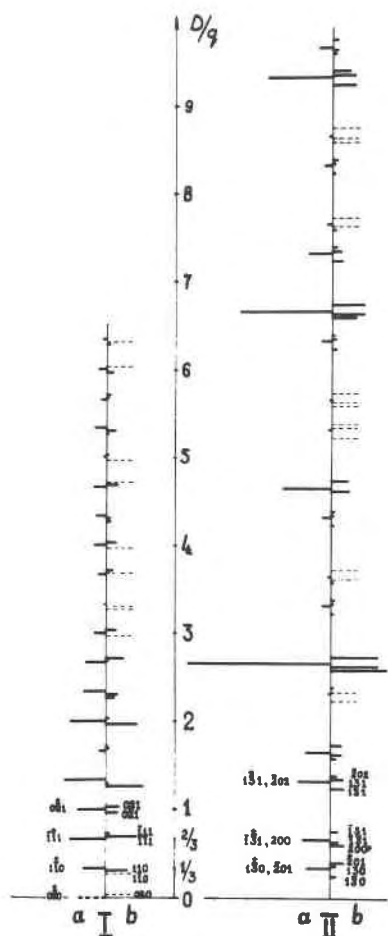


FIG. 2. Schemes of reflection distributions along the first (I) and second (II) ellipses of the cookeite oblique texture pattern in cases of $p/q = 1/3$, $s = 0$ (a) and $p/q = 0.297$, $s/q = 0.016$ (b). The line lengths are taken proportional to F^2 values; dotted lines indicate theoretical positions of reflections not revealed experimentally.

genetic significance of this di,triocahedral chlorite polytype.

The cookeite studied formed during a late stage of bauxite transformation, reconstructed as follows. Following metamorphic and, later, tectonic action, the bauxite strata developed local zones of intensive, fine jointing. Silica-rich solutions circulated along these fine joints and reacted with the alumina of the bauxite to form pyrophyllite. The formation of pyrophyllite may indicate that rather high P, T parameters existed during the mineral genesis and also that alkaline cations were absent from the solutions. The formation of the structurally perfect di,triocahedral chlorite cookeite occurred in the zones of later tectonic shears in the pyrophyllite mass

as a result of the interaction of new Li-rich solutions with pyrophyllite.

It should also be noted that the pyrophyllite formed not only along macrojoints but also inside the bauxite mass along microslacking zones (zones where microcracks—splits, clefts, fissures—are abundant). This is proved by the presence of cookeite admixed with pyrophyllite in bauxite, though in this case the cookeite is not so structurally perfect as in tectonic slacking zones. According to petrographic and X-ray data, the emery in the bauxite contains an appreciable amount of hematite and a small amount of corundum. On these grounds one can reasonably suggest that iron is essentially absent in the processes. Thereby the absence of the noticeable isomorphous replacements of Fe for Al, that is natural for pyrophyllite and cookeite, is observed.

References

- BAILEY, S. W., AND B. E. BROWN (1962) Chlorite polytypism: I. Regular and semi-random one-layer structures. *Am. Mineral.* **47**, 819–850.
- BRINDLEY, G. W., BERYL OUGHTON, AND K. ROBINSON (1950) Polymorphism of the chlorites. I. Ordered structures. *Acta Crystallogr.* **3**, 408–416.
- BROWN, B. E., AND S. W. BAILEY (1963) Chlorite polytypism: II. Crystal structure of a one-layer Cr-chlorite. *Am. Mineral.* **48**, 42–61.
- DRITS, V. A., AND V. A. ALEXANDROVA (1968) Structure of mineral from donbassite group—dioctahedral chlorite from New Land. *Mineral. Collect. Lvov Univ.* **22**, 162–167.
- , AND E. K. LASARENKO (1967) Structurally-mineralogical features of donbassites. *Mineral. Collect. Lvov Univ.* **21**, 40–48.
- LISTER, JUDITH S., AND S. W. BAILEY (1967) Chlorite polytypism: IV: Regular two-layer structures. *Am. Mineral.* **52**, 1614–1631.
- MATHIESON, A. MCL., AND G. F. WALKER (1954) Crystal structure of magnesium-vermiculite. *Am. Mineral.* **39**, 231–255.
- SHIROZU, HARUO, AND S. W. BAILEY (1966) Crystal structure of a two-layer Mg-vermiculite. *Am. Mineral.* **51**, 1124–1143.
- STEINFINK, H. (1958a) The crystal structure of chlorite. I. A monoclinic polymorph. *Acta Crystallogr.* **11**, 191–195.
- (1958b) The crystal structure of chlorite. II. A triclinic polymorph. *Acta Crystallogr.* **14**, 198–199.
- ZVYAGIN, B. B. (1963) The theory of chlorite polymorphism. *Kristallografiya*, **8**, 32–38.
- (1967) *Electron-Diffraction Analysis of Clay Mineral Structures*. Plenum Press, New York.
- , K. S. MISHENKO, AND S. V. SOBOLEVA (1968) The structures of pyrophyllite and talc in the light of polytypism of micalike minerals. *Kristallografiya*, **13**, 599–604.
- , A. F. FEDOTOV, S. V. SOBOLEVA, AND K. S. MISHENKO (1972) The reflection of monoclinic angle of layer silicates in the electron diffraction oblique texture patterns. *Kristallografiya*, **17**, 851–853.

Manuscript received, August 29, 1974; accepted for publication, April 28, 1975.